ISSN 2321-807X
Volume 12 Number11
Journal of Advances in Chemistry

Photoluminescence, laser damage threshold, optical transmittance, FTIR, mechanical, dielectric, thermal and XRD studies on Bis – Glycine hydrochloride single crystal

L. Gobinathan[a,*] and K. Boopathy[b]

[a] Department of Physics, VSA Group of Institution, Salem, Tamil Nadu, India.

[b] Department of Physics, Govt. Engineering College, Dharmapuri, Tamil Nadu, India.

Abstract

Single crystals of Bis – glycine hydrochloride (BGHC) were grown from aqueous solution by means of slow evaporation and slow cooling techniques. Single crystal XRD study reveals that the grown BGHC crystallizes in orthorhombic system with space group $P2_12_12_1$ and the obtained unit cell parameters are a = 5.32 Å, b = 8.10 Å and c = 18.01 Å. Powder X – ray diffraction pattern of grown BGHC has been indexed. Functional groups present in the BGHC crystals were identified by FT – IR spectral analysis. The transmission and absorption spectra for the grown BGHC crystal shows that the lower cut off wavelength lies at 235 nm. The photoluminescence spectrum of the grown crystal was recorded. Mechanical hardness of the grown BGHC was determined and Vickers microhardness hardness number was calculated. Laser damage threshold study was carried out for the grown crystal using Nd:YAG laser. The thermal stability of the grown crystal was investigated using thermogravimetric analysis and the grown crystal is thermally stable up to 198 °C. Particle size dependent second harmonic generation efficiency of the grown crystal was examined by Kurtz and Perry powder technique using 1064 nm laser.

Keywords: Growth from solution, Infrared spectroscopy, Photoluminescence, Laser damage threshold, Nonlinear optical materials.

*Corresponding Author Tel. No: +91 - 8190908999

E – Mail id: (L. Gobinathan)

1. Introduction

Recent years, molecular based second order nonlinear optical crystals have attracted much interest because of their potential applications in emerging optoelectronic technologies. Much effort have been made to develop the new materials with high second order nonlinearities and are expected to underpin applications in the areas such as electro-optic switching for telecommunication, optical information processing, optical data storage and generation of terahertz radiation [1 – 3]. The halogenides and metal halogenides of glycine, their structural and physical properties have attracted extensive interest in material chemistry. Glycine is the simplest amino acid. Unlike other amino acids it has no asymmetric carbon and is optically inactive. It has three polymeric crystalline forms α, β and γ [4, 5]. Both α and β forms crystalline in centrosymmetric space group $P2_1/c$ [6, 7], γ – glycine crystallizes in non – centrosymmetric space group $P3_1$ [8, 9]. While glycine can exist as the neutral molecules the gas as phase, it exists as zwitterions in solution and in the solid state. Numerous complexes of glycine halogenides were reported. It was reported that glycine combines hydrochloride [10], hydrobromide [11], hydroiodide [12], disarcosine hydrobromide [13], hydrofluoride [14] and nitrate [15]. The crystal structure of diglycine hydrochloride was determined and reported by Hahn and Buerger [16] with orthorhombic system and space group $P2_12_12_1$. BGHC crystal is a suitable candidate for nonlinear optical (NLO) application. Ambujam et.al [17] has reported growth and characterization of grown single crystals of bis – glycine hydrochloride in gel media and slow evaporation method. In the present work we have attempted to grow the crystals from both slow evaporation and slow cooling techniques. In the present investigation, the grown crystals were characterized by X - ray diffraction analysis, Fourier transform infrared spectroscopy, UV – Vis – NIR optical absorption and transmission, microhardness, photoluminescence, laser damage threshold, dielectric studies, thermal and nonlinear optical properties.

2. Experimental

2.1 Materials Synthesis

Commercially available glycine (AR grade) and hydrochloric acid (AR grade) was used for synthesis BGHC salt. The solution was prepared in the molar ratio of 2:1in double distilled water at room temperature. BGHC salt was obtained by the evaporation of the solvent at 40ºC and then it was purified by repeated recrystallization process. The material thus prepared was used to grow bulk BGHC crystals. Bisglycine hydrochloride salt is synthesized according to the following reaction

$$2(NH_2CH_2COOH) + HCl \rightarrow (NH_3^+CH_2COO^-)(NH_3^+CH_2COOH)Cl^-$$

ISSN 2321-807X
Volume 12 Number11
Journal of Advances in Chemistry

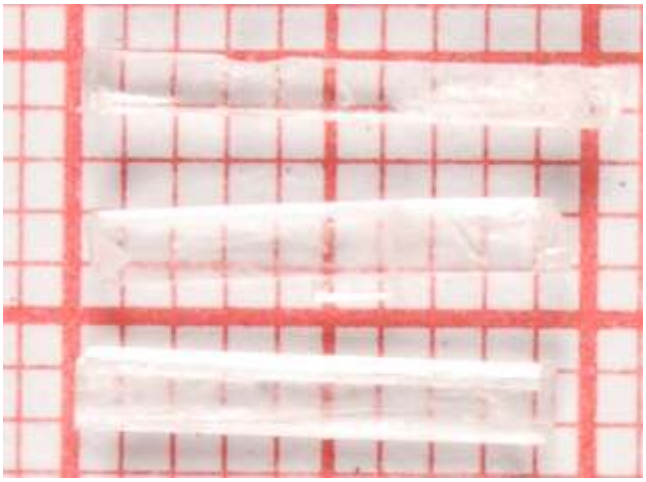

Fig.1 (a) As grown BGHC single crystals by slow evaporation technique

2.2 Crystal growth

BGHC crystals were grown from slow cooling method in a constant temperature bath having an accurate of ± 0.01 °C. A good transparent optically quality single crystal obtained by slow evaporation method at room temperature was selected as a seed crystal and is shown in Fig. 1(a). This selected seed crystal was used to initiate the crystal growth process by suspending the seed crystal in the solution saturated at 40 °C. Following the slow cooling method the temperature of the constant temperature bath was reduced from 40 °C at a rate of 0.1 °C per day. The grown crystal of size 9 mm x 4 mm x 3 mm was harvested after a growth period of 7 days and the grown crystals are shown in Fig. (1b).

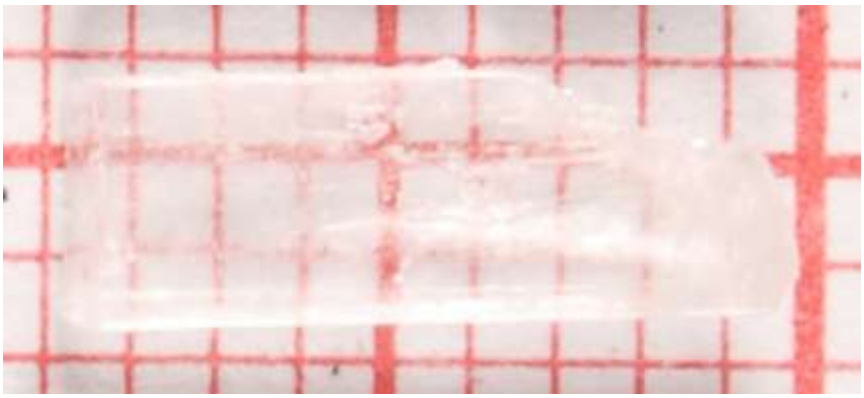

Fig.1 (b) As grown BGHC single crystals by slow cooling method

3. Result and discussion

3.1 X – ray diffraction studies

Single crystal X - ray diffraction analysis was carried out by Bruker Nonius CAD 4 single crystal X - ray diffractometer using Cu Kα radiation (λ = 1.5405 Å). The unit cell parameters are obtained and it is in good agreement with the reported [18] values and thus confirms the grown crystal. The obtained crystal data are given in Table 1. BGHC crystallizes in orthorhombic system and space group $P2_12_12_1$, which is recognized as non – centrosymmetric, thus satisfying one of the basic and essential criteria for the SHG efficiency of the crystal [19].

Powder X - ray diffraction study was carried out by employing SEIFERT JSO DEBYEFLEX (Model 2002) diffractometer using Cu Kα radiation (λ = 1.5405 Å). The powdered sample was scanned over the range of 20 - 80º at a scanning rate of 1º/ min. From the powder XRD data the various planes of reflections were indexed using the software AUTOX 93. The indexed X - ray diffraction patterns are shown in Fig.2. The X – ray diffraction pattern has the highest intensity corresponding to the (021) plane.

ISSN 2321-807X
Volume 12 Number11
Journal of Advances in Chemistry

Table 1 Unit cell parameters of BGHC single crystal

Parameters	Single crystal X – ray diffraction	
	Present study	**Reported values [18]**
a	5.32 Å	5.3094 Å
b	8.10 Å	8.1159 Å
c	18.01 Å	17.9527 Å
α, β & γ	90°	90°
Volume	774.8 $Å^3$	773.5859 $Å^3$
Crystal system	Orthorhombic	Orthorhombic
Space group	-	$P2_12_12_1$

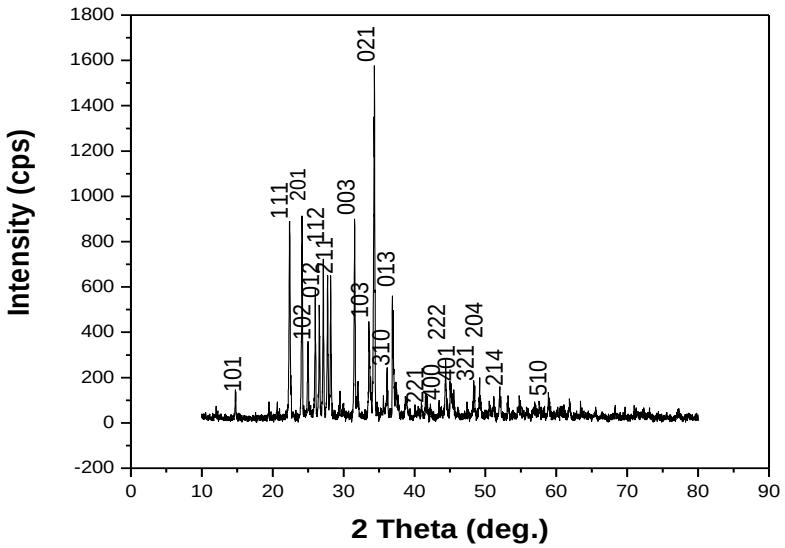

Fig.2 Powder X – ray diffraction pattern of BGHC

3.2 FT - IR spectral studies

BGHC single crystal FT - IR spectrum was recorded at 300 K by Perkin Elmer FT - IR spectrophotometer using KBr pellet technique. The characteristic absorption peaks are observed in the range of 400 - 4000 cm^{-1} as shown in Fig.3. The very strong band absorbed at 1720 cm^{-1} is due to C = O stretching vibration of COOH group. The band observed at 1589 and 1498 cm^{-1} are assigned to NH_3^+ asymmetric and symmetric bending vibrations, respectively. The peak at 1247 cm^{-1} is due to the C = O in plane bending vibration of carboxylic acid group. The intense sharp peak at 1330 cm^{-1} is due to the CH_2 wagging vibration. The broad band around 1023 cm^{-1} indicates that the characteristic frequencies of CN stretching vibration. The strong peak at 667 cm^{-1} is attributed to COO^- bending vibration. The peak at 583 and 508 cm^{-1} are assigned to COO^- wagging and rocking vibrations, respectively. Frequency assignment of the absorption peaks are presented in Table 2, which is in good agreement with the reported work [20].

ISSN 2321-807X
Volume 12 Number11
Journal of Advances in Chemistry

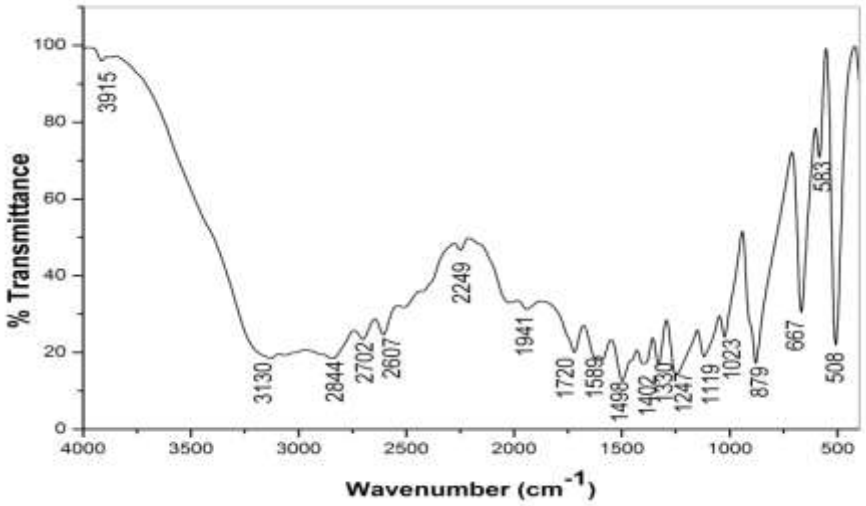

Fig. 3 FTIR spectrum of BGHC single crystal

Table 2 Tentative vibrational band assignments of BGHC single crystals

BGHC	BGHC [20]	Band assignments
3915	-	O - H Asymmetric stretching
3130	-	O - H Symmetric stretching
1941	-	combinational band
1720	1720	C = O stretching of - COOH
1589	1591	NH_3^+ asymmetric bend
1498	1501	NH_3^+ symmetric bend
1402	1409	CH_2 scissoring vibration
1330	1336	CH_2 wagging vibration
1247	1253	C = OH in plane bending of - COOH
1119	1112	NH_3^+ rocking vibration
1023	1028	CN stretching vibration
879	874	C – C stretching vibration
667	673	COO^- bending vibration
583	581	COO^- wagging vibration
508	504	COO^- rocking vibration

3.3 UV – Vis - NIR spectrum

The UV – Vis – NIR spectrum gives limited information about the structure of the molecule because the absorption of UV and visible light involves promotion of the electron in σ and π orbital's from the ground state to higher state [21]. Transmission spectra are very important for any NLO materials because a nonlinear optical material can be of practical use only if it has wide transparence window. UV – Vis – NIR transmittance spectrum of BGHC was recorded in the range of 190 - 1100 nm using Varian Cary 5E UV – Vis – NIR spectrophotometer and is shown in Fig. 4. For optical device fabrications, the crystal should be highly transparent in the considerable region of wavelength. From the graph, it is evident that the grown crystal is transparent in the entire visible region, suggests its suitability for second harmonic generation (SHG) efficiency. The UV absorption edge for the grown BGHC is found to be 235 nm, which is sufficiently low for SHG laser radiation at 1064 nm or other application in the blue region [22]. The dependence of optical absorption coefficient with the photon energy helps to study the band structure and the type of the transition of electrons. The optical absorption coefficient (α) was calculated from the transmittance spectral data using the following relation,

$$\alpha = \frac{1}{t}\log\left(\frac{1}{T}\right) \quad (1)$$

where, T is the transmittance and t is the thickness of the crystal. Owing to the direct band gap, the crystal under study has an absorption coefficient (α) obeying the following relation for high photon energies (hυ),

$$\alpha = \frac{A(h\upsilon - Eg)^{1/2}}{h\upsilon} \quad (2)$$

where, E_g is the optical band gap of the crystal and A is a constant. The plot of variation of $(\alpha h\upsilon)^2$ versus hυ is shown in Fig. 5. Band gap energy of the grown crystal (E_g) is evaluated by the extrapolation of the linear part. The calculated band gap energy of the grown crystal is ~ 5.46 eV. As a consequence of wide band gap, the grown crystal has large transmittance in the visible region. The optical behavior of the materials is important to determine its usage in optoelectronic devices.

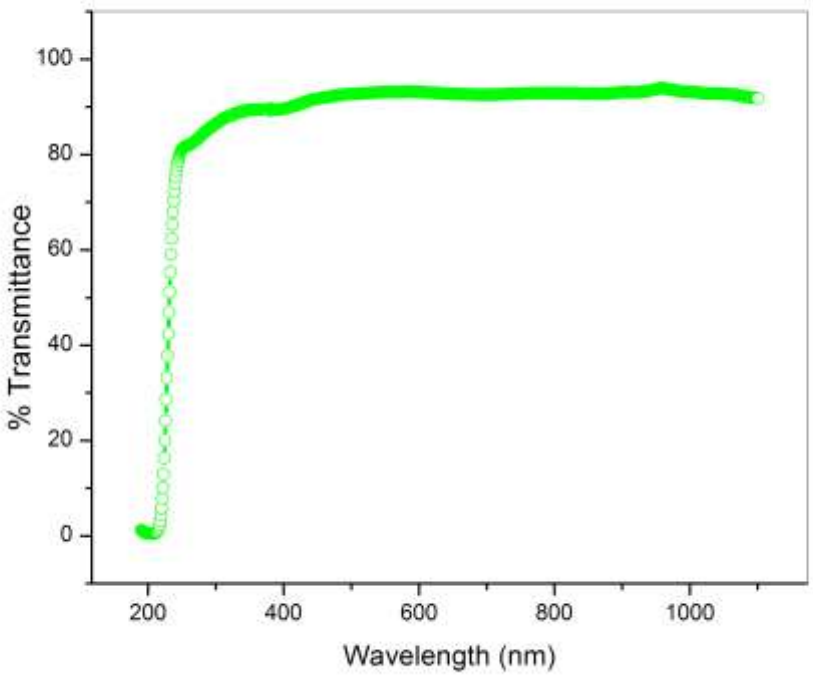

Fig. 4 UV – Vis – NIR transmittance spectrum of BGHC

Knowledge of optical constant of a material such as optical band gap energy and extinction coefficient is quite essential to examine the materials potential for optoelectronic applications. Where α is the absorption coefficient and it is related to extinction coefficient (K). K is determined by

ISSN 2321-807X
Volume 12 Number11
Journal of Advances in Chemistry

$$K = \frac{\alpha\lambda}{4\pi} \qquad (3)$$

Figure 6 show the variation of extinction coefficient (K) as a function of wavelength and it is clear that extinction coefficient depend on the absorption coefficient. The internal efficiency of the device also depends on the absorption coefficient. Hence, by tailoring the absorption coefficient, one can achieve the desired material to fabricate the optoelectronic devices.

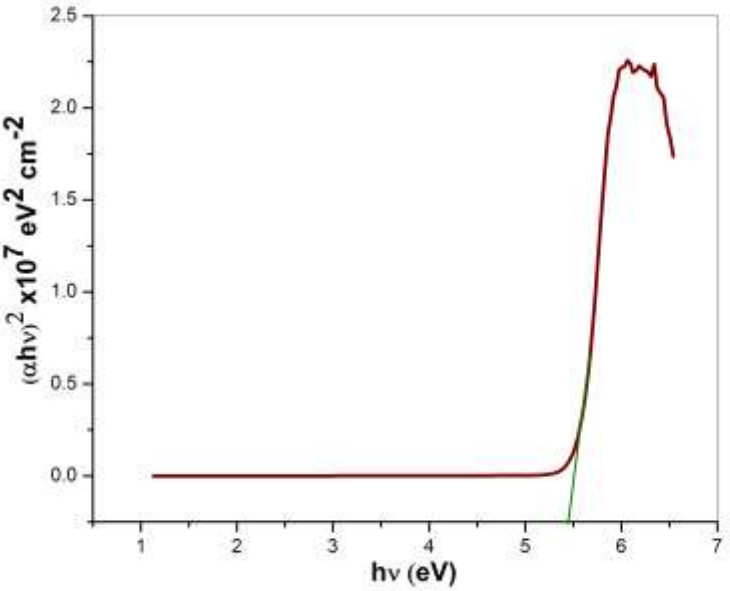

Fig. 5 Plot of $(\alpha h\upsilon)^2$ vs. photon energy for BGHC

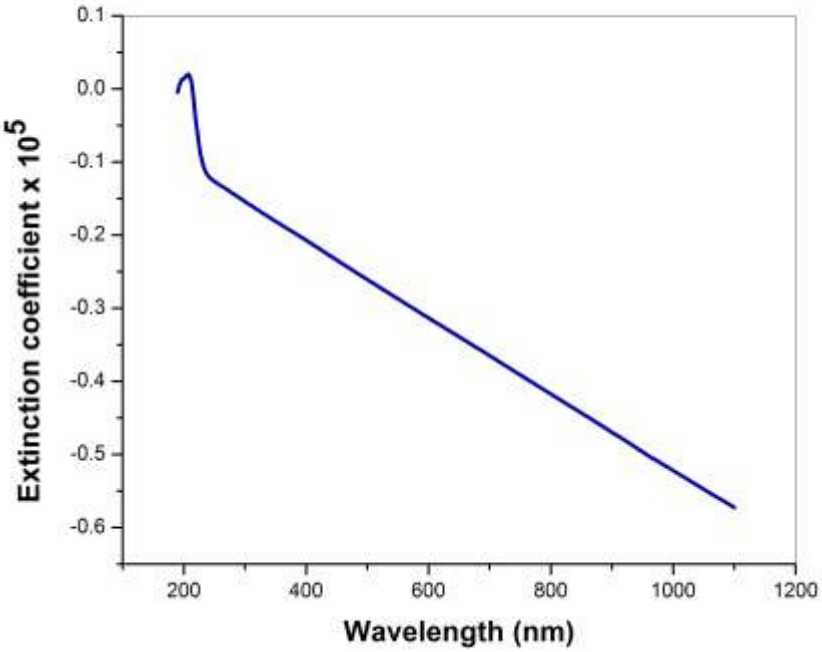

Fig. 6 Plot of extinction coefficient (K) vs. wavelength of BGHC

3.4 Vickers microhardness studies

Microhardness measurements were carried out on BGHC crystal using Vickers HMV 2000 microhardness tester fitted with a diamond pyramidal indentor. The measurements were done at room temperature for different forces. The indentations were made using a Vickers pyramidal indenter for various loads from 25g, 50g and 100g. The diagonals of the impression were measured using shimadzu Vickers microhardness tester. Vickers microhardness number (H_v) was evaluated using the following relation

$$H_v = \frac{1.8544P}{d^2} kg/mm^2 \qquad (4)$$

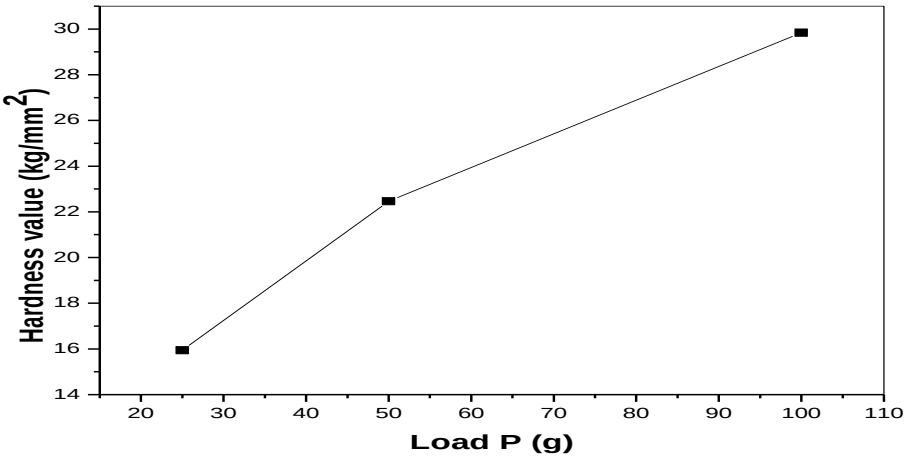

Fig. 7 Hardness behavior of BGHC

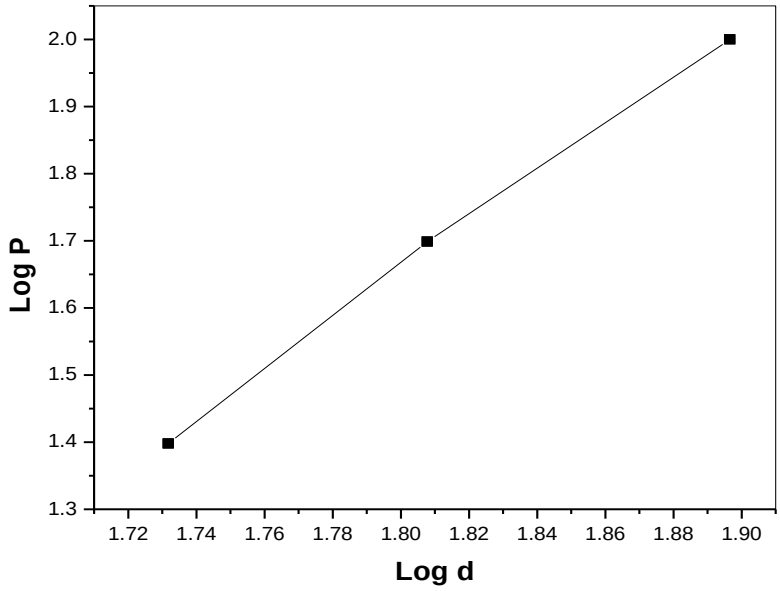

Fig. 8 Meyers plot for BGHC single crystal

where, H_v is the Vickers microhardness number, P is the applied load and d is the diagonal length of the indentation impression. The variation of microhardness values with applied load is shown in Fig. 7. Hardness values are found to increases with increasing applied loads. For a load of more than 100g, cracks started developing around the indentation mark which may be due to the release of internal stresses. The variation of H_v with load for BGHC increases and reaches a saturation values at higher loads. Such a phenomenon is referred to as the reverse indentation size effect (RISE) [23]. In

order to analyze the ISE in the hardness testing, one needs to fit the experimental data according to Meyer's power law, which correlates the applied test load P and indentation size d

$$P = Ad^n \quad (5)$$

where, n is the Meyer's index (or) work hardening co – efficient and A is the material constant. In the present work the plot obtained between log P and log d gives a straight line. The work hardening coefficient (n) was calculated from Fig. 8 by the least square curve fitting method. The value of n for BGHC is 4.2, so the BGHC falls under the soft material category.

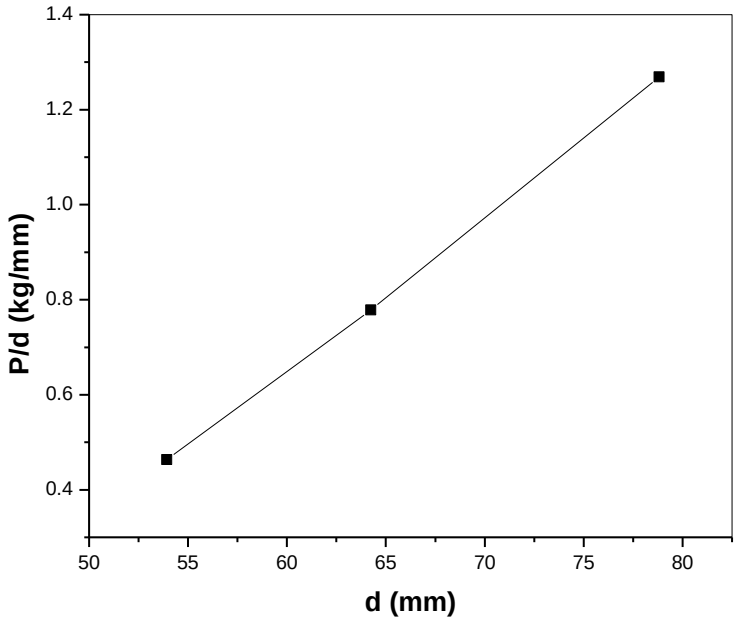

Fig.9 PSR plot of P/d vs. d for BGHC

Onitsch [24] inferred that a value of n lies between 1 and 1.6 for hard materials and for soft materials it is above 1.6. To explain the ISE, PSR model, microhardness can be described with two components, the first term represents the resistance of the test material against elastic deformation and the second term represents the load independent part. The indentation load P is related to indentation size of as

$$P = a_1 d + a_2 d^2 \quad (6)$$

The above equation can be rearranged as $p/d = a_1 (P_0/d_0^2)\, d_0$. Li and Bradt [25] explained the indentation size effect with the proportional specimen resistance (PSR) model. PSR model describes the ISE regime and load independent part. A plot of p/d against d will give a straight line, the slope of which gives the value of load independent microhardness value for BGC single crystal (Fig.9). The slope value of p/d^2 multiplied by the Vickers conversion factor 1.8544 gives 55.6 g/mm^2 for the value of the load independent microhardness. In this present study the calculated load independent microhardness value for BGHC is 55.6 g/mm^2.

3.5 Dielectric studies

Dielectric properties are correlated with the electro – optic property of the crystal [26]. Carefully discerned samples of BGHC were cut and polished on a soft tissue paper. The sample was electrode on both sides with silver paste to make the sample behave as a parallel plate capacitor. The sample dimension 4 × 3 × 3 mm^3 was used for this experiment. A HIOKI 3635 model LCR meter was used to measure the capacitance (C) and dissipation factor (D) of the sample as a function of frequency. A small cylindrical furnace, whose temperature was controlled by a Eurotherm temperature controller (0.01 °C) was used to house the sample. The dielectric constant was calculated by using the relation $\varepsilon_r = Cd/(A\varepsilon_0)$, where ε_0 is the permittivity of free space, t is the thickness of the crystal, C is the capacitance and A is the area of the cross section. The dielectric loss was calculated using the relation $\varepsilon'' = \varepsilon_r D$, where D is the dissipation factor. The result of dielectric constant and loss measurement are shown in Fig. 10 and 11. It can be reasoned out that the dielectric constant and loss value decrease with increase of frequency. The large value of dielectric constant at low frequency suggest that there is a contribution from all four know sources of polarization namely, electronic, ionic, dipolar and space charge polarization.

ISSN 2321-807X
Volume 12 Number11
Journal of Advances in Chemistry

Space charge polarization is generally active at lower frequencies and high temperatures and indicates the perfection of the crystals [27]. Further, the space charge polarization will depend on the purity and perfection of the material.

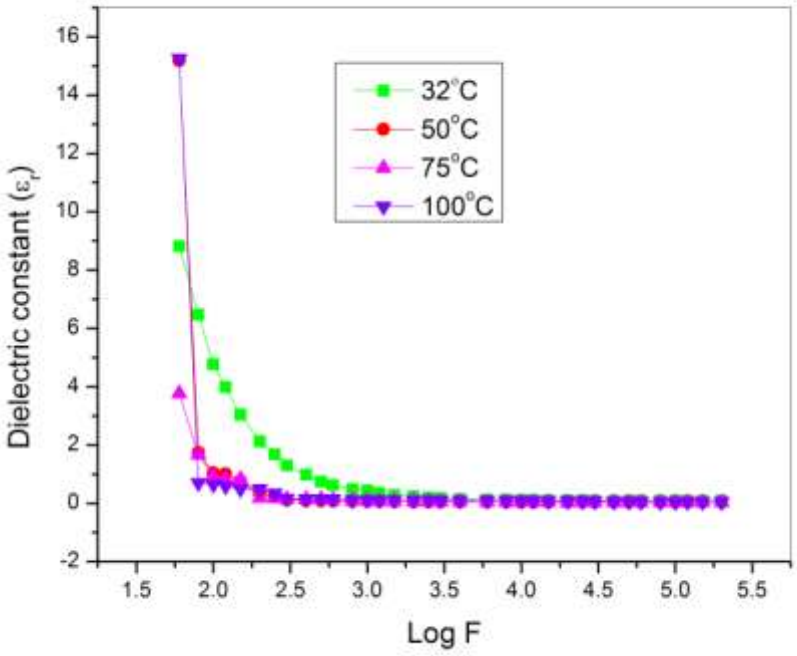

Fig. 10 Dielectric constant vs. log F for BGHC

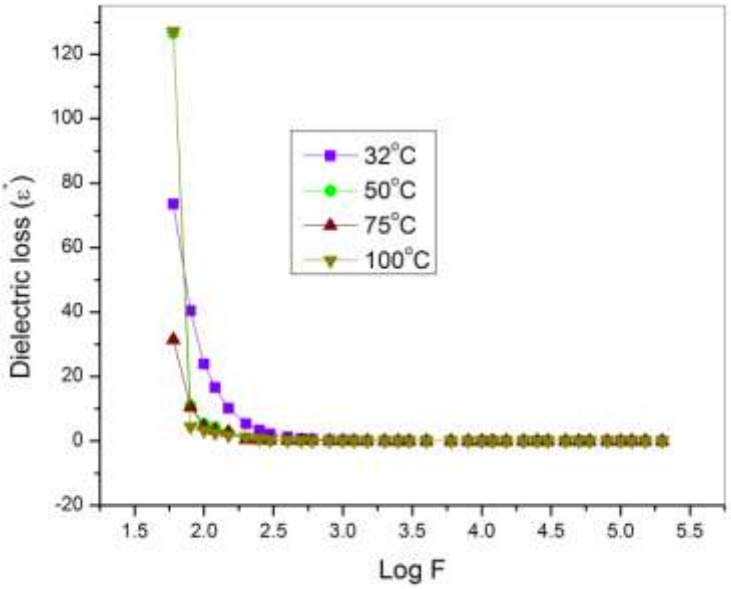

Fig. 11 Dielectric loss vs. log F for BGHC

3.6 Photoluminescence study

Photoluminescence (PL) is a powerful tool for investigating the energy levels of materials. It is also one of the most effective tools for providing important information about the physical properties of materials at the molecular level,

including shallow and deep level defects and gap – states [28]. Figure 12 shows the room temperature PL spectrum of BGHC crystal, which is excited at 300 nm. The donor – acceptor type and ionic property of the grown crystal may give rise to luminescence. The broad photoluminescence emission peak seen in the spectra at 445 nm is due to interaction between the electronic system of the luminescent centre and the vibrations of ions which have it. Such a broad emission was caused by derive electronic transitions occurring in different energy levels due to deep or shallow holes within the band gap. In the present study, broad PL emission at 445 nm violet emission is an indicative of the charge transfer process as well as the trapping of electrons and it is due to the contribution of the shallow holes than the deep holes. Thus, PL emission spectrum revealed that BGHC crystal exhibits blue shift emission, which is most useful for luminescent applications.

3.7 Laser damage threshold study

Laser damage threshold in optical materials refers to permanent damage caused by melting, ablation, cracking, plasma formation etc., when an optical material exposed to laser radiation. Laser damage threshold of the optical materials are getting an important role due to high optical intensities involved in nonlinear process and it must withstand to high power intensities [29]. For laser damage threshold experiment, the Q – switched 1064 nm Nd:YAG pulsed laser was used. The laser beam profile with repetition rate of 10 Hz and pulse width of 8 ns was used. The flat surface of the crystal was polished and subjected to laser damage threshold measurement. The polishing technique of the materials produces minimum subsurface damage and it can be raised the surface damage threshold. The rear surface damages occurred due to Fresnel reflection loss at the front surface result in less energy [30]. The multishot laser damage threshold measurement was made on the BGHC with 1 mm beam spot. The output intensity of the laser was controlled with variable attenuator and delivered on the surface of the sample located at the near focusing of the converging lens. The energy density of the laser beam was noted for which the crystal gets damage. The surface laser damage threshold of BGHC crystal was calculated using $P(d) = E/\tau A$, where E is the intensity of the incident laser beam (mJ), τ is the pulse width (ns) and A is the area of the circular spot size (cm^2). The calculated laser damage threshold value of BGHC crystal is found to be 1.62 GW/cm^2. From this LDT result, it is observed that the BGHC crystal is potential material for optical applications.

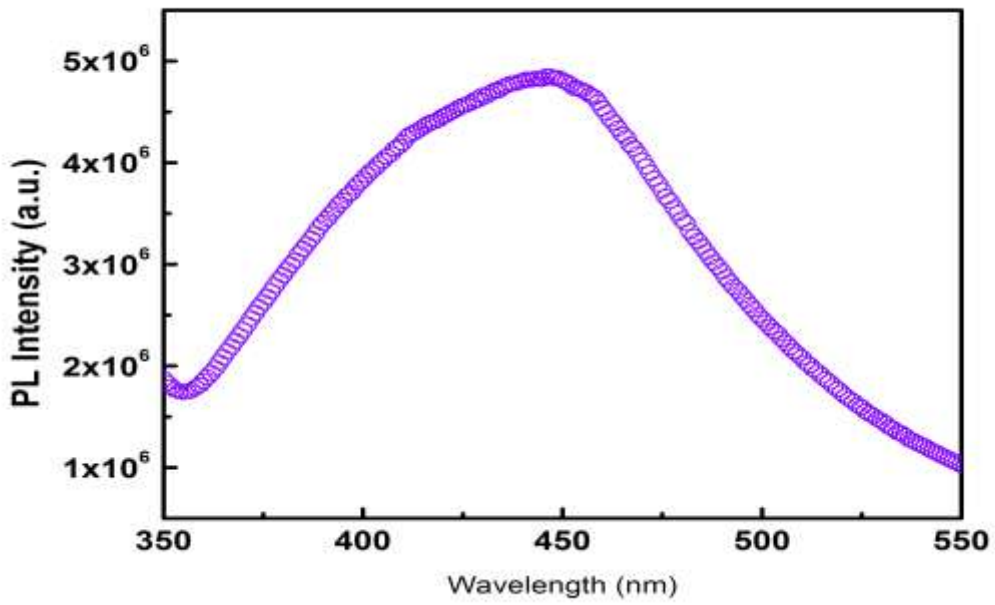

Fig. 12 Photoluminescence spectrum of BGHC

3.8 Thermal analyses

Thermogravimetric analysis (TGA) was carried out using a SDT Q600 V8.3 instrument in the temperature range of 55 to 1000 °C at a heating rate of 10 °C / min in a nitrogen gas atmosphere. The grown crystal was crushed into fine powder and TGA and DTA trace were recorded in the temperature range from 55 to 1000 °C. Fig.13 shows the TGA and DTA spectra of BGHC crystal with three stages of weight loss. There is no loss of weight below 198 °C indicating the absence of any absorbed water in the sample. In the first step of decomposition starts at 198 °C and ends at 285 °C resulting in a weight loss of 40 % of the total weight of the material taken. This step of decomposition is due to the loss of one glycine molecule. The second step of weight loss takes place between the temperature 285 °C and 720 °C. In the second stage of weight loss takes place the removal of another one glycine molecule. Third step of decomposition is observed between the temperature 720 °C and 980 °C.

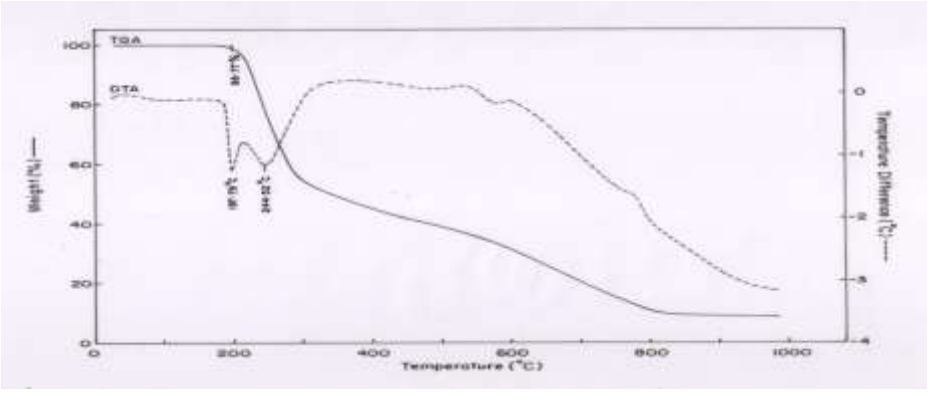

Fig.13 TGA / DTA trace of BGHC single crystals

During this stage of decomposition one chlorine molecule is removed. In addition to that DTA curve shows an endothermic peck at 197 °C and 244 °C for BGHC crystal respectively. The sharp peak observed at 197 °C is due to the melting point of the compound. The powder form of a single crystal of BGHC was filled in a micro-capillary tube which was placed in the melting point apparatus (GUNA make). The temperature was increased slowly and the melting of the material was observed at 195 °C.

3.9 Kurtz powder SHG test

Quantitative measurement of relative SHG efficiency of BGHC and well – known SHG material of KDP was used by the Kurtz and Perry [31] powder technique. A laser beam of fundamental wavelength of 1064 nm Q – switched Nd:YAG laser radiation, 8 ns pulse width with 10 Hz pulse rate was used. In the present study, the crystalline powder was sieved into different particle size ranges such as 100, 120, 140, 160 and 180 µm. The KDP samples were used as reference for the second harmonic generation test. The ground BGHC and KDP samples were loaded into uniform bore glass micro-capillaries, which is having a inner diameter of about 600 µm. The sample was placed to 1064 nm monochromatic radiation and green signal was observed from the sample. It confirms the capacity of frequency conversion (SHG) efficiency of BGHC single crystal. The intensity of the green signal was detected by a photomultiplier tube and displayed on a storage oscilloscope. The output SHG signal voltages of the different sized powdered samples were observed to be 150, 165, 184, 198 and 236 mV for 100, 120, 140, 160 and 180 µm respectively. It is observed that the SHG intensities increase with increase in particle size (Fig. 14). The relative SHG efficiency of BGHC is about 3.0 times that of KDP at about 180 µm. This strongly suggests the grown crystal as a potential candidate for SHG applications.

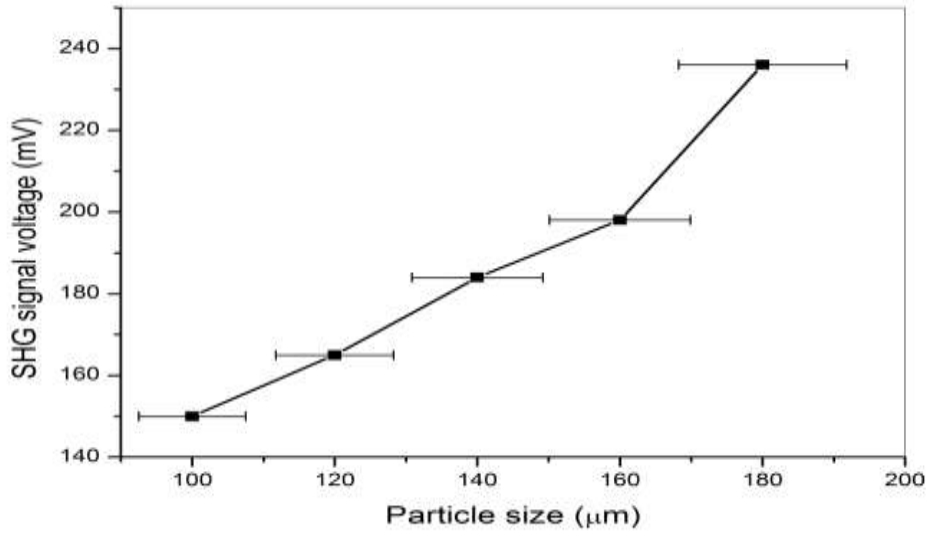

Fig. 14 Kurtz powder SHG signal voltage vs. particle size

4. Conclusion

Bulk single crystals of Bis - glycine hydrochloride (BGHC) were grown successfully by slow evaporation and slow cooling method using double distilled water as solvent. Single crystal X – ray diffraction study reveals that the grown crystal belongs to orthorhombic system with space group $P2_12_12_1$. Good crystallinity of the grown material is confirmed by the appearance of sharp peaks in the PXRD pattern of BGHC. FT – IR spectroscopic analysis revealed the functional groups present in the grown crystal. BGHC molecule occurs in the zwitter ion configuration, while both the amino group and carboxyl group are protonated. But the BGHC molecules have a positive ion with the charge formally residing on the NH_3^+. Due to this reason BGHC can be act as a nonlinear polarizability and hence exhibit nonlinear optical properties. The lower cut off wavelength is observed at 235 nm from UV – Vis – NIR transmittance spectrum in the range of 235 – 1100 nm. The absence of absorption in the entire visible region make BGHC single crystal a potential NLO material for second harmonic generation in the visible region especially in the blue and violet light region. The band gap energy for the grown crystal was found to be 5.46 eV. The Vickers hardness values increases with increasing load and the crystal experiences cracks for loads above 100g. Photoluminescence spectral studies suggest that strong charge transfer occurs in the molecule. Laser damage threshold efficiency of BGHC crystal is 1.62 GW/cm^2. The decomposition stages were analyzed from thermal analyzes and found that the melting point is 195 °C; hence, it suggests the application limit. The SHG property was analyzed for different particle size by Kurtz and Perry method and found that SHG intensity increases with increase in particle size. From the characterization results, it is observed that the BGHC crystal is potential material for optical applications.

References

[1] G.G.A. Balavoine, J.C. Daran, G. Iftime, P.G. Lacroix, E. Manoury, J.A. Delaire, I.M. Fanton, K. Nakatani, S. D. Bella, Synthesis, crystal structure and second order nonlinear optical properties of new chiral ferrocenyl materials, Organometallic, 18 (1999) 21 – 29.

[2] H.O. Mercy, L.F. Warren, M.S. Webb, C.A. Ebbers, S.P. Velsko, G.C. Kennedy, G.C. Catella, Second harmonic generation in zinc tris (thiourea) sulfate, Appl. Opt. 31 (1992) 5051 – 5060.

[3] L. Li, H. Cui, Z. Yang, X. Tao, X. Lin, N. Ye, H. Yang, Synthesis and characterization of thienyl – substituted pyridinium salts for second order nonlinear optics, Cryst. Eng. Comm. 14 (2012) 1031 – 1037.

[4] M. Narayan Bhat, S.M. Dharmaprakash, New nonlinear optical material: glycine sodium nitrate, J. Crystal Growth 235 (2002) 511 - 516.

[5] T. Balakrishnan, K. Ramamurthi, Structural, thermal and optical properties of a semiorganic nonlinear optical single crystal: Glycine zinc sulphate, Spectrachim. Acta part A 68 (2007) 360 – 363.

[6] Ra. Shanmugavadivu, G. Ravi, A. Nixon Azariah, Crystal growth, thermal and optical studies of nonlinear optical material: Glycine potassium sulphate, J. Phy. & Chem. Solids 67 (2006) 1858 - 1861.

[7] G. Albrecht, R.B. Corey, The crystal structure of Glycine, J. Am. Chem. Soc. 61 (1939) 1087

[8] Y. Iitaka, The crystal structure of γ – glycine, Acta Cryst. 11 (1958) 225

[9] Y. Iitaka, The crystal structure of γ – glycine, Acta Cryst. 14 (1961) 1

[10] S. Natarajan, C. Muthukrishnan, S. A. Bahadur, R. K. Rajaram, S. S. Rajan, Reinvestigation of the crystal structure of diglycine hydrochloride, Z. Kristallogr. 198 (1992) 265

[11] M. J. Buerger, R. Barney, T. Hahn, The crystal structure of diglycine hydrobromide, Z. Kristallogr. 108 (1956) 130

[12] P. Piret, J. Meunier – Piret, J. Verbist, M. Van Meerssche, Bull. Soc. Chim. Belg. 81 (1972) 539

[13] S. C. Bhattacharyya, N. N. Saha, Crystal and molecular structure of disarcosine hydrobromide, J. Cryst. Mol. Struct. 8 (1978) 209

[14] K. Selvaraju, R. Valluvan, S. Kumararaman, New nonlinear optical material: Glycine hydrofluoride, Materials Letters 60 (2006) 2848 - 2850.

[15] R. kanagadurai, R. Sankar, G. Sivanesan, S. Srinivasan, R. Rajassekaran, R. Jayavel, Growth and characterization studies of ferroelectric diglycine nitrate (DGN) single crystal, Material Chem. & Phys. 108 (2008) 170 – 175.

[16] T. Hahn, M. J. Buerger, The crystal structure of diglycine hydrochloride 2($C_2H_5O_2N$). HCl, Z. Krist. 108 (1957) 419.

[17] K. Ambujam, K. Rajarajan, S. Selvakumar, I. vethapotheher, Ginson P. Joseph, P. Sagayaraj, Growth and characterization of a novel NLO crystal bis - glycine hydrogenchloride, J. Crystal Growth 286 (2006) 440 - 444.

[18] B. Narayana Moolya, S.M. Dharmaprakash, Nonlinear optical diglycine hydrochloride: Synthesis, crystal growth and structural characteristics, J. Cryst. Growth, 293 (2006) 86 – 92.

[19] J. Zyss, J. F. Nicoud, M. Coquillay, Chirality and hydrogen bonding in molecular crystals for phase-matched second harmonic generation: N- (4-nitrophenyl)-(L)-prolinol (NPP), J. Chem. Phys. 81 (1984) 4160

[20] K. Ambujam, K. Rajarajan, S. Selvakumar, J. Madhavan, Gulam Mohamed, P. Sagayaraj, Growth and characterization of gel grown single crystals of bis-glycine hydrogen chloride (BGHC), Optical Materials 29 (2007) 657 – 662.

[21] R. Sankar, C.M. Raghavan, M. Balaji, R. Mohan Kumar, R. Jayavel, Synthesis and growth of Triauaglycinesulfato zinc (II), $[Zn(SO_4)(C_2H_5NO_2)(H_2O)_3]$, a new semiorganic nonlinear optical crystal, Cryst. Growth & Design, 7 (2007) 348

[22] S. Selvakumar, S.M. Ravi Kumar, K. Rajarajan, A. Joseph Arul Pragasam, S.A. Rajasekar, K. Thamizharasan and P. Sagayaraj, Growth and characterization of a novel organometallic nonlinear optical crystal: Bis(Thiourea) cadmium Formate, Cryst. Growth & Design, Vol.7, No.11, (2006) 2607 – 2610.

[23] F. Frohlich, P. Grau, W. Wrellmann, Performance and analysis of recording microhardness tests, Phys. Status Solid 42 (1977) 79 – 82.

[24] E. M. Onitsch, Mikroskopie – 2 (1947) 131 - 151.

[25] H. Li, R. C. Bradt, Knoop microhardness anisotropy of single crystal LaB_6, Mater. Sci. Engine. A 142 (1991) 51

[26] S. Boomadevi, R. Dhanasekaran, Synthesis, crystal growth and characterization of L – Pyrrolidone – 2 carboxylic acid (L – PCA) crystals, J. Cryst. Growth 261 (2004) 70 – 76.

[27] N. V. Prasad, G. Prasad, T. Bhimasankaran, S. V. Suryanarayan, G. S. Kumar, Indian J. Pure Appl. Phys. 34 (5), (1996) 639.

[28] D. K. Schroder, Semiconductor material and device characterization, New York, John Wiley, 1990.

[29] G. C. Bhar, A. K. Chaudhary, P. Kumbhakar, Study of laser induced damage threshold and effect of inclusions in some nonlinear crystals, Appl. Surf. Sci. 161 (2000) 155 – 162.

[30] H. L. Bhat, Growth and characterization of some novel crystals for nonlinear optical applications, Bull. Mater. Sci. 17 (1994) 1233 – 1249.

[31] S. K. Kurtz, T. T. Perry, A powder technique for the evaluation of nonlinear optical materials, J. Appl. Phys. 39 (1968) 3798 – 3813.